GEOPHYSICAL RESEARCH LETTERS, VOL. 21, NO. 16, PAGES 1667-1670, AUGUST 1, 1994

Rapid determination of global moment-tensor solutions

Stuart A. Sipkin

U.S. Geological Survey, MS 967, Box 25046, DFC, Denver, CO 80225

Abstract. In an effort to improve data services, the National Earthquake Information Center has begun a program, in cooperation with the Incorporated Research Institutions for Seismology Data Management Center (IRIS DMC), to produce rapid estimates of the seismic moment tensor for most earthquakes with a body-wave magnitude of 5.8 or greater. Although this program is still undergoing testing and fine-tuning, an estimate of the moment tensor can usually be produced within 20 minutes of the arrival of the broadband *P*-waveform data from the IRIS DMC. Although the speed with which this data can be obtained varies, in many cases a solution can be obtained within two hours of the earthquake. These solutions do not vary significantly from the final solutions determined using the entire network. Because of the manner in which the data and the synthetic seismograms are aligned, the method is insensitive to the effects of timing errors, epicentral mislocation, and lateral heterogeneity in earth structure. This procedure was implemented in May 1993; the results from that month are presented here.

Introduction

Because of the proliferation of so-called "open" seismic stations, those with either satellite telemetry or dial-up capability, there now exists an unprecedented opportunity to analyze high-quality digitally-recorded broadband seismic data in real or near-real time. This has lead to several schemes for the rapid determination of earthquake source mechanisms using both teleseismic [*Ekström*, 1992, 1993; *Giardini*, 1992] and regional [*Ritsema and Lay*, 1993; *Romanowicz et al.*, 1993] data. The aforementioned procedures for determining the seismic moment tensor from teleseismic data are based upon the Centroid-Moment Tensor (CMT) formalism developed by *Dziewonski et al.* [1981]. This method has been exceptionally successful in the effort to comprehensively catalog earthquake mechanisms over a wide range of earthquake size. One of the reasons for the success of this method is its use of long segments of the seismogram, including several circuits of the surface waves for larger events, that have been low-pass filtered, with a corner period of 45 s for the body waves and 135 s for the surface waves. The use of long time series can, however, in many cases mean waiting several hours after the occurrence of an event to analyze the data.

In order to minimize the interval between the occurrence of an earthquake and the time when the necessary data have been received, we are utilizing the method developed by *Sipkin* [1982], using only the *P*-waveforms (including depth phases). The main catalysts for this development are the U.S. National Seismograph Network (USNSN) in the conterminous United States and the Global Telemetered Seismograph Network (GTSN) in the southern hemisphere, operated by the U.S. Geological Survey (USGS), and the Global Seismograph Network (GSN), operated by the USGS and the University of California at San Diego in cooperation with the Incorporated Research Institutions for Seismology (IRIS). The data that are most readily accessible are the four minutes of broadband data that are saved to the ring buffers of the open IRIS/GSN stations, and the real-time broadband data from the USNSN, with a trigger window of six minutes. Given these limitations, an inversion of only the *P*-waveforms is possible.

Paper number 94GL01429
0094-8534/94/94GL-01429$03.00

Procedure

The flow of data is as follows. An automatic process at the National Earthquake Information Center (NEIC), using real-time data from the USNSN and the GTSN, identifies phase arrivals, associates the data, and computes an origin time and hypocenter. This information is sent by e-mail to the IRIS Data Management Center (DMC) where it triggers the SPYDER data retrieval system. The four minutes of broadband data containing the *P*-wave arrival are retrieved from the ring buffers of the open IRIS/GSN stations, shown in Figure 1, and transmitted to the NEIC over the Internet. These data are merged with the USNSN/GTSN data set and used to refine the origin time and hypocenter and to compute a body-wave moment tensor. This solution is then broadcast by e-mail to any interested parties.

The method of inversion is based on the theory of optimal filter design and is fully described by *Sipkin* [1982, 1986*a*,*b*]. Since this method was designed to work best using long-period teleseismic data the broadband waveforms are first low-pass filtered, with a corner period of 20 s. The source-time function is assumed to be a step function at the source. This can lead to a bias in the estimated scalar moment for moments larger than approximately 10^{20} Nm.

As a part of the data preprocessing all of the *P*-wave arrivals are temporally aligned, and during inversion the synthetic seismograms are similarly aligned, thus eliminating the effects of timing errors, epicentral mislocation, and lateral heterogeneity. The moment tensor is constrained to be purely deviatoric (zero trace), but not a pure double couple (zero determinate). Since this constraint is linear, for any particular depth the inversion is linear. The focal depth is determined by finding the depth that minimizes the normalized mean-square-error between the real and synthetic data. For earthquakes with a depth greater than about 40 km this usually results in a very accurate depth estimate because of the prominence of the depth phases. For example, Figure 2 shows the real and synthetic waveforms from the 27 May intermediate-depth (~120 km) earthquake in the Kermadec Islands. This earthquake is deep enough that the depth phases combine to form a complex waveform, but shallow enough that they are not well separated. For earthquakes with a depth greater than about 40 km this usually results in a formal uncertainty on the order of 2–3 km; for shallower focal depths the merging of the primary arrival and the depth phases results on a somewhat greater uncertainty, on the order of 5 km. Since the estimated focal depth is highly model dependent, the true uncertainties are greater, probably by a factor of two.

Application

We began applying this procedure routinely in May 1993. The origin times and hypocentral parameters of the eleven events ana-

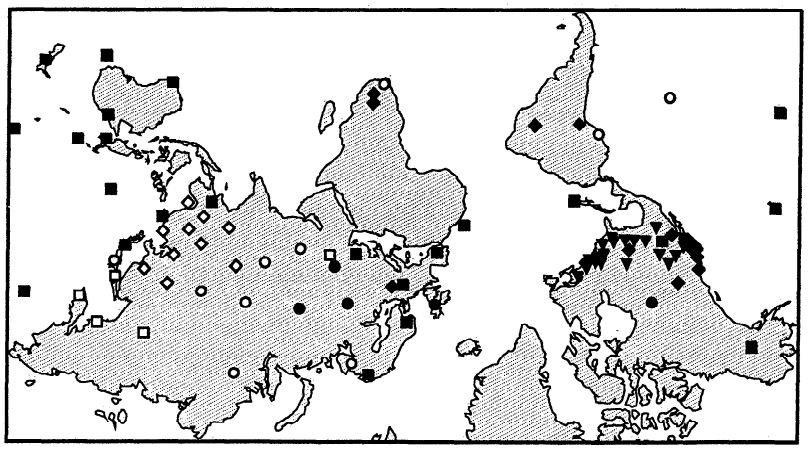

Figure 1. Digitally-recording broadband seismograph stations used. Triangles, squares, circles, and diamonds show the locations of USNSN, IRIS/USGS, IRIS/IDA, and other stations, respectively. Filled symbols indicate stations for which real-time, or near real-time, data is available; open symbols indicate stations that are available for later analysis.

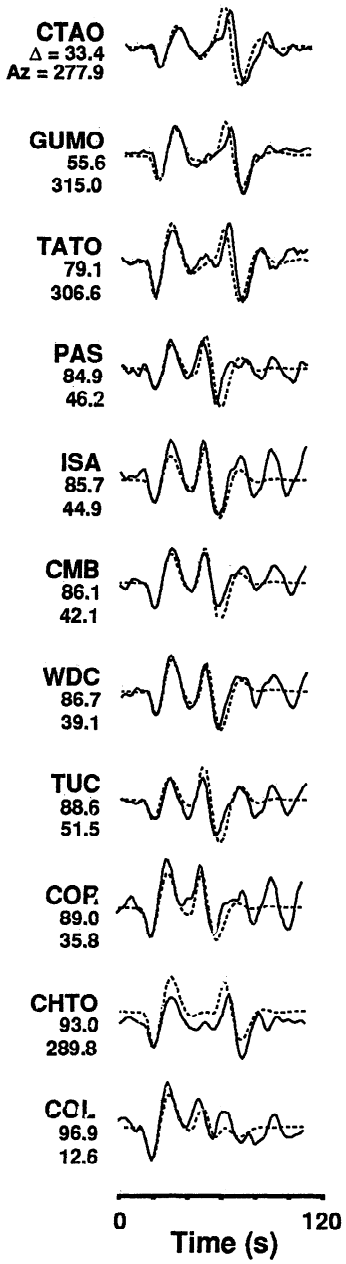

lyzed that month are given in Table 1 and the epicenters and best double-couples are shown in Figure 3.

Because of the growing number of open digital seismograph stations, these preliminary solutions should be very similar to those produced later, using data from the entire network (Figure 1). We demonstrate this by comparing the various solutions in Figure 4 and Table 2. All of the mechanisms shown in Figure 4 are very stable, with the possible exception of the 27 May Kermadec Islands event (no. 11). Because of its location and smaller size this event had a rather poor initial station distribution, which substantially improved when the rest of the network became available. In general, both the focal depth and scalar moment also appear to be very stable, as demonstrated in Table 2. The scalar moments derived from the fast and final moment tensors do not differ by more than a factor of two, and for most events are much closer and, with the exception of event no. 5, the differences in focal depth do not exceed 8 km. The differences between the fast moment tensor and the final CMT depths are somewhat larger, although part of this difference, as well as those in mechanism and scalar moment, may be explained by the differing frequency bands being used [*Tanioka et al.*, 1993], as well as differences in the earth models used.

Table 1. Hypocentral Parameters

Date (1993)	Time (UTC)	Lat (°)	Long (°)	Depth (km)	m_b	M_S
2 May	11:26:55	−56.4	−24.5	13	6.3	6.4
6 May	13:03:18	−8.5	−71.5	573	5.8	
11 May	18:26:51	7.2	126.6	59	6.1	6.6
13 May	11:59:49	55.2	−160.5	32	6.4	6.8
15 May	21:52:25	51.4	−178.7	32	6.2	6.6
17 May	16:02:53	−5.3	152.0	17	5.7	6.3
17 May	23:20:49	37.2	−117.8	7	6.0	6.0
18 May	10:19:34	19.9	122.4	169	6.4	
24 May	23:51:28	−22.7	−66.5	221	6.6	
25 May	23:16:43	55.0	−160.5	37	6.2	5.8
27 May	08:51:59	−29.4	−178.3	118	5.9	

Figure 2. Waveforms from the 27 May intermediate-depth (~120 km) earthquake in the Kermadec Is. Solid lines are the real data, dashed lines are the synthetic seismograms. Epicentral distance and source-receiver azimuth are indicated below the station name.

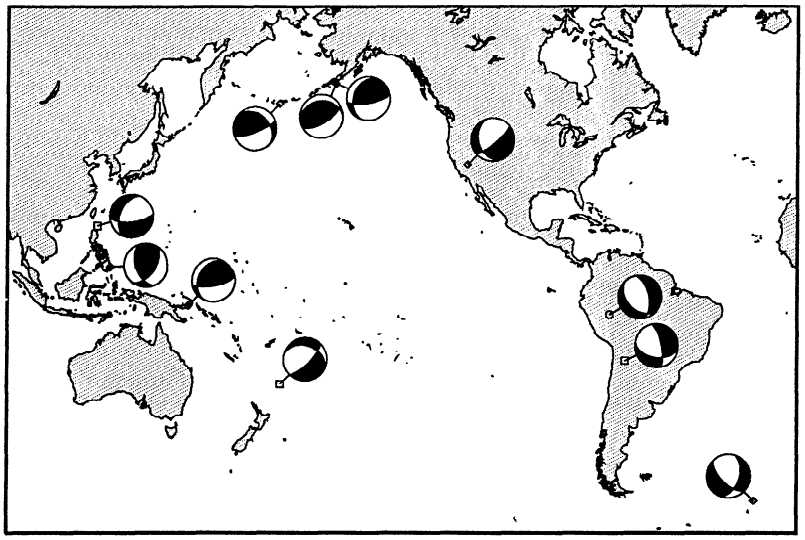

Figure 3. Epicenters and best double-couples of May 1993 earthquakes for which a fast moment-tensor solution was determined. Diamonds, squares, and circles show the epicenters of shallow- (0–70 km), intermediate- (70–300 km), and deep- (300–700 km) focus events, respectively. Compressional quadrants are shaded.

Conclusions and Future Directions

Using the first four-to-six minutes of waveform data that is rapidly available immediately after an earthquake, we are able to quickly and accurately compute the mechanism, size, and depth of the event. The procedure works well for most earthquakes with body-wave magnitudes of 5.8 or greater, and smaller in some cases. For events with a scalar moment of greater than 10^{20} Nm we plan to improve estimates of moment by introducing a more realistic source duration.

One of the goals of this project is to more fully automate the system and to decrease the response time. For example, when this work was initiated, each seismogram that went into the inversion was first screened to determine its suitability. Based upon accumulated knowledge, a simple signal-to-noise ratio threshold was established to automatically reject unsuitable waveforms. The success of this procedure, *i.e.* discarding the same waveforms as would an analyst, has shortened the analysis time. The part of the procedure that still requires analyst intervention is making sure that the depth found does not occur at a local minimum in the normalized mean-square-error vs. depth. This is most likely to happen when the initial depth issued in the NEIC alert is off by more than about 20 km. Occasionally, such a minimum is of the same order as that at the "true" depth, requiring a visual inspection

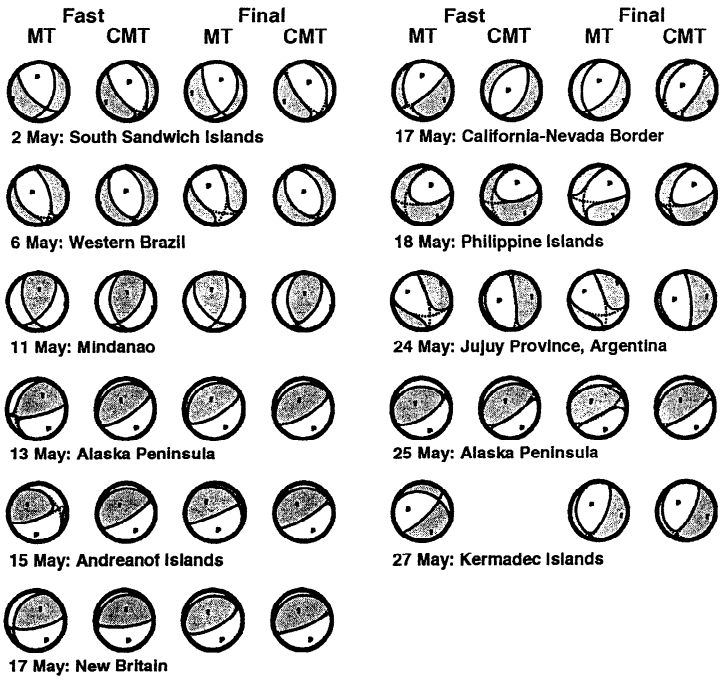

Figure 4. Comparison of rapidly determined moment-tensor solutions with those determined using the entire network. Solid curves show the nodes of the moment tensor, dashed curves show the nodal planes of the best double-couple solutions. Compressional quadrants are shaded.

Table 2. Comparison of Source Parameters

Date (1993)	Region	Depth (km)					*Mo* (Nm)			
		Fast		Final			Fast		Final	
		MT†	CMT‡	BB§	MT†	CMT‡	MT†	CMT‡	MT†	CMT‡
2 May	So. Sandwich Is.	15	15	13	14	15	$4.3\cdot10^{18}$	$5.4\cdot10^{18}$	$4.4\cdot10^{18}$	$5.1\cdot10^{18}$
6 May	Western Brazil	574	588	573	568	595	$2.9\cdot10^{18}$	$2.0\cdot10^{18}$	$1.5\cdot10^{18}$	$1.8\cdot10^{18}$
11 May	Mindanao, PI	40	46	59	43	46	$4.0\cdot10^{19}$	$3.5\cdot10^{19}$	$3.8\cdot10^{19}$	$3.4\cdot10^{19}$
13 May	Alaska Peninsula	25	38	32	29	41	$2.3\cdot10^{19}$	$2.5\cdot10^{19}$	$2.3\cdot10^{19}$	$2.5\cdot10^{19}$
15 May	Andreanof Is.	42	17	32	25	26	$1.4\cdot10^{19}$	$2.3\cdot10^{19}$	$2.0\cdot10^{19}$	$2.5\cdot10^{19}$
17 May	New Britain	23	28	17	16	23	$4.4\cdot10^{18}$	$4.2\cdot10^{18}$	$3.1\cdot10^{18}$	$4.5\cdot10^{18}$
17 May	Calif-Nevada Bord.	11	15	7	8	15	$1.7\cdot10^{18}$	$1.2\cdot10^{18}$	$1.6\cdot10^{18}$	$1.8\cdot10^{18}$
18 May	Philippine Is.	180	178	169	177	188	$1.4\cdot10^{19}$	$1.0\cdot10^{19}$	$2.0\cdot10^{19}$	$1.3\cdot10^{19}$
24 May	Jujuy Province	222	229	221	222	232	$3.3\cdot10^{19}$	$3.5\cdot10^{19}$	$3.3\cdot10^{19}$	$3.3\cdot10^{19}$
25 May	Alaska Peninsula	31	45	37	39	49	$2.4\cdot10^{18}$	$1.5\cdot10^{18}$	$1.9\cdot10^{18}$	$1.5\cdot10^{18}$
27 May	Kermadec Islands	120		119	116	128	$9.1\cdot10^{17}$		$5.3\cdot10^{17}$	$5.2\cdot10^{17}$

†MT: USGS moment tensor
‡CMT: Harvard CMT
§BB: USGS Broad-band body-wave depth

of the waveform fit. Work is progressing on automating this part of the procedure as well.

The largest bottleneck in the system is the wait for the IRIS data. It currently takes approximately two hours from the time of the event to receive this data. Personnel at the NEIC and the IRIS DMC are working on ways to decrease this time lag. Hopefully, at some future time, all broadband digital stations will have near-real-time telemetry; at that time, procedures for rapidly determining source parameters can replace the routine procedures now being employed some four months after the event.

Acknowledgments.. I thank Madeleine Zirbes for helping with the software development and Jim Dewey, Bob Engdahl, Hitoshi Kawakatsu, Thorne Lay, and Larry Ruff for reviewing the manuscript. This would not have been possible without the cooperative efforts of the personnel at the NEIC and the IRIS DMC. In particular, I thank Tim Ahern, Ray Buland, and Steve Malone for making this work.

References

Dziewonski, A.M., T.A. Chou, and J.H. Woodhouse, Determination of earthquake source parameters from waveform data for studies of global and regional seismicity, *J. Geophys. Res., 86*, 2825–2852, 1981.

Ekström, G., Quick CMTs – What's the next step? (abstract), *4th Annual IRIS Workshop*, April 12–14, Santa Fe, New Mexico, 1992.

Ekström, G., Rapid earthquake analysis at Harvard, *IRIS Newsletter*, XII, 4–6, 1993.

Giardini, D., Moment tensor inversion from MedNet data: (1) Large worldwide earthquakes of 1990, *Geophys. Res. Lett., 19*, 713–716, 1992.

Ritsema, J., and T. Lay, Rapid source mechanism determination of large ($M_W \geq 5$) earthquakes in the western United States, *Geophys. Res. Lett., 20*, 1611–1614, 1993.

Romanowicz, B., D. Dreger, M. Pasyanos, and R. Uhrhammer, Monitoring of strain release in central and northern California using broadband data, *Geophys. Res. Lett., 20*, 1643–1646, 1993.

Sipkin, S.A., Estimation of earthquake source parameters by the inversion of waveform data: Synthetic waveforms, *Phys. Earth Planet. Inter., 30*, 242–259, 1982.

Sipkin, S.A., Interpretation of non-double-couple earthquake source mechanisms derived from moment tensor inversion, *J. Geophys. Res., 91*, 531–547, 1986*a*.

Sipkin, S.A., Estimation of earthquake source parameters by the inversion of waveform data: Global seismicity, 1981–1983, *Bull. Seismol. Soc. Amer., 76*, 1515–1541, 1986*b*.

Tanioka, Y., L. Ruff, and K. Satake, Unusual rupture process of the Japan Sea earthquake, *EOS, 74*, 377–380, 1993.

S.A. Sipkin, U.S. Geological Survey, MS 967, Box 25046, DFC, Denver, CO 80225. (email: sipkin@gldfs.cr.usgs.gov)

(Received: February 25, 1994; accepted: April 7, 1994)